

MANTLE PYROXENITIC "LIQUIDS" AND "CUMULATES": GEOCHEMISTRY OF COMPLEX XENOLITHS FROM SAN CARLOS, KILBOURNE'S HOLE AND EASTERN AUSTRALIA

Anthony J. Irving (The Lunar Science Institute, 3303 NASA Rd. 1, Houston, Texas 77058)

Mantle-derived xenoliths in alkalic basalts may be subdivided into several distinct series, the most common of which are the Cr-diopside spinel lherzolite series and the Al-Ti-augite series (eg. Wilshire and Shervais, 1975; Wass and Irving, 1976). Both series are mineralogically and texturally diverse. Rocks of both series commonly occur together, but nearly always as separate xenoliths showing no structural relationship to each other. At some localities, however, rare composite xenoliths are found which display the structural relationships among at least some members of each series.

Previous geochemical studies, especially trace element studies, of Al-Ti-augite series rocks have utilized discrete xenoliths (eg. Frey and Prinz, 1977; Irving, 1974). This paper is primarily concerned with the geochemistry of Al-Ti-augite-rich rocks which have an observable relationship to Cr-diopside spinel lherzolite or harzburgite. Most of the analyzed samples take the form of dikes or veins intruding or enclosing lherzolite or harzburgite. These structures imply that these particular Al-Ti-augite-rich rocks were mobile (probably liquid) at high pressures whereas adjacent lherzolite and harzburgite were more rigidly solid (cf. Wilshire and Shervais, 1975). Two discrete Al-Ti-augite series xenoliths showing poikilitic texture were also analyzed.

The following samples were studied:

Wehrlite SC74-1W and harzburgite SC74-1H, San Carlos, Arizona. A composite sample showing angular clasts of harzburgite enclosed and veined by black wehrlite to produce a "xenolith-in-xenolith" structure (see Fig. 1a).

Wehrlite dike SH76-2P and adjacent Cr-diopside spinel lherzolite SH76-2L, Sapphire Hill, north Queensland, Australia. An exceptionally large composite specimen showing a 6 cm wide dike of wehrlite with double contacts against spinel lherzolite (see Fig. 1b).

Wehrlite dike SC73-2 cutting spinel lherzolite, San Carlos. A 2 cm wide dike of wehrlite showing double contacts against spinel lherzolite.

Websterite dike KH73-1 cutting spinel lherzolite, Kilbourne's Hole, New Mexico. A 5 cm wide branched dike showing double contacts against fine grained, weakly foliated spinel lherzolite.

Wehrlite dike KH76-1 cutting more olivine-rich wehrlite, Kilbourne's Hole.

Part of a network of 3 cm wide dikes and 0.5 cm wide anastomosing veins cutting coarse grained more olivine-rich Al-Ti-augite-bearing wehrlite (see Fig. 1c).

Wehrlite SD72-1 enclosing spinel lherzolite, Mt. Shadwell, Victoria, Australia.

A composite sample displaying "xenolith-in-xenolith" structure (see Fig. 1d). The wehrlite contains areas of fine grained vesicular "basaltic" material which do not appear to be connected to the enclosing basalt.

Poikilitic wehrlites SC73-3 and SC73-6, San Carlos. Two similar samples (grainsize 5 mm) composed of olivine enclosed poikilitically by Al-Ti-augite and spinel. The textures are those of adcumulates. These samples are richer in olivine than any of the other analyzed wehrlites.

Major and trace element data (by XRF and INAA) for these materials are reported in Tables 1 and 2, and REE patterns are shown in Figs. 2 and 3. The pyroxene-rich "liquids" show a range in composition. 100 Mg/Mg+Fe ranges from 85 down to 75, but the largest variation is in Cr (44 to 3250 ppm). Chon-

drite-normalized REE patterns for most of these samples are characterized by depletion in light REE relative to Sm. Except for SH76-2P, they are also depleted in heavy REE relative to Sm. One sample (SD72-1) is light REE enriched. The two poikilitic wehrlites have similar REE patterns to the other wehrlites but at somewhat lower abundances. Spinel lherzolite SH76-2L is enriched in both light and heavy REE relative to Sm, Eu and Tb, like some examples from San Carlos and Victoria (Frey and Prinz, 1977; Frey and Green, 1974).

A popular interpretation of Al-Ti-augite-rich xenoliths is that they represent re-equilibrated cumulates from alkalic basaltic magmas at high pressures (10-20 kb). Most of the present samples were evidently entirely molten or crystal-liquid mushes at high pressures, yet their REE patterns are similar to those predicted for high pressure cumulates from magmas like their present hosts (Frey and Prinz, 1977). At mantle pressures, gravity crystal settling may be insignificant because of the difficulty of holding large magma chambers open. However, a process of flow crystallization within dikes like those described here could produce rocks chemically indistinguishable from settled cumulates. High-pressure fractionation of basanitic magmas to yield hawaiitic to phonolitic liquids (eg. Irving and Green, 1976) may well take place by such processes.

References

- Frey, F.A. and Green, D.H. (1974) The mineralogy, geochemistry and origin of lherzolite inclusions in Victorian basanites. Geochim. Cosmochim. Acta, **38**, 1023-1059.
- Frey, F.A. and Prinz, M. (1977) Ultramafic inclusions from San Carlos, Arizona: Petrologic and geochemical data bearing on their petrogenesis. Earth Planet. Sci. Lett. (in press).
- Irving, A.J. (1974) Pyroxene-rich ultramafic xenoliths in the Newer Basalts of Victoria, Australia. Neues Jb. Miner. Abh., **120**, 147-167.
- Irving, A.J. and Green, D.H. (1976) Geochemistry and petrogenesis of the Newer Basalts of Victoria and South Australia. J. Geol. Soc. Aust., **23**, 45-66.
- Wass, S.Y. and Irving, A.J. (1976) XENMEG: a catalogue of occurrences of xenoliths and megacrysts in basic volcanic rocks of Eastern Australia. Spec. Publ. Aust. Museum, 455 p.
- Wilshire, H.G. and Servais, J.W. (1975) Al-augite and Cr-diopside ultramafic xenoliths in basaltic rocks from western United States. Physics and Chemistry of the Earth, **9**, p. 257-272.

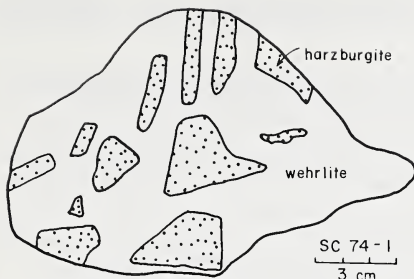


FIG. 1 (a)

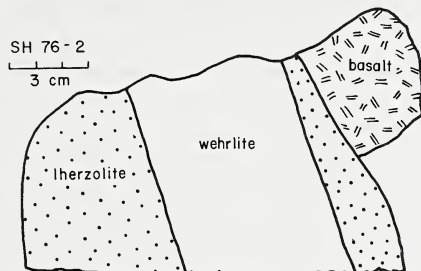


FIG. 1 (b)

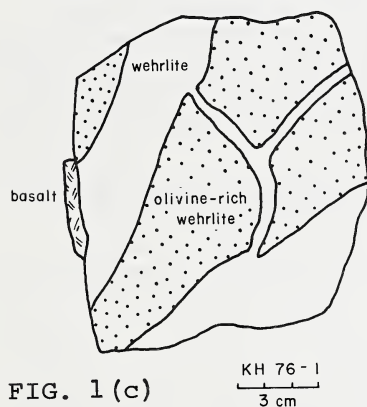


FIG. 1 (c)

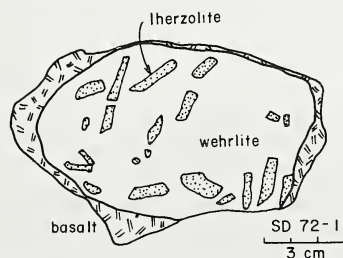


FIG. 1 (d)

Table 1. Major element data (By XRF, except * by IMA)

| | Wehrlite SC74-1W | Wehrlite SH76-2F | Wehrlite SC73-2 | Wehrlite KH73-1 | Wehrlite KH76-1 | Wehrlite SD72-1 | Harzburgite SC74-1H | Spinel Lherzolite SH76-2L | Poikilitic Wehrlite SC73-3 | Poikilitic Wehrlite SC73-6 |
|----------------------------------|---------------------|---------------------|--------------------|--------------------|--------------------|--------------------|------------------------|---------------------------------|----------------------------------|----------------------------------|
| SiO ₂ | 52.07 | 47.29 | 43.03 | 42.26 | 42.31 | 47.89 | 42.33 | 44.28 | 40.15 | 41.90 |
| TiO ₂ | 0.45 | 0.46 | 1.94 | 1.22 | 1.54 | 1.39 | 0.18 | 0.08 | 0.42 | 0.57 |
| Al ₂ O ₃ | 4.83 | 10.12 | 13.33 | 15.45 | 13.53 | 4.48 | 1.43 | 2.48 | 3.84 | 3.32 |
| Cr ₂ O ₃ * | 0.47 | 0.34 | 0.10 | 0.006 | 0.016 | 0.19 | 0.35 | 0.36 | 0.16 | 0.16 |
| FeO | 9.27 | 6.17 | 6.62 | 6.51 | 9.11 | 7.49 | 13.56 | 9.03 | 15.16 | 14.09 |
| MnO | 0.20 | 0.16 | 0.18 | 0.17 | 0.20 | 0.18 | 0.21 | 0.17 | 0.26 | 0.25 |
| MgO | 28.01 | 20.21 | 16.92 | 15.36 | 15.45 | 17.10 | 40.06 | 40.09 | 33.01 | 30.87 |
| SiO ₂ * | 0.08 | 0.07 | 0.08 | 0.05 | 0.04 | 0.06 | 0.26 | 0.25 | 0.18 | 0.16 |
| CaO | 3.30 | 13.58 | 16.19 | 18.11 | 15.98 | 16.07 | 0.72 | 1.90 | 5.47 | 7.60 |
| Na ₂ O* | 0.290 | 0.67 | 1.11 | 0.82 | 1.12 | 1.37 | 0.089 | 0.102 | 0.387 | 0.409 |
| P ₂ O ₅ | 0.02 | 0.01 | 0.08 | 0.01 | 0.02 | 0.55 | 0.01 | 0.01 | 0.04 | 0.01 |
| F ₂ O ₅ | 0.01 | 0.02 | 0.03 | 0.00 | 0.01 | 0.20 | 0.00 | 0.04 | 0.00 | 0.00 |
| Sum | 99.20 | 99.30 | 99.61 | 99.97 | 99.33 | 99.37 | 99.40 | 99.19 | 99.08 | 99.34 |
| 100 Mg | | | | | | | | | | |
| Mg+Fe | 84.3 | 85.4 | 82.0 | 80.8 | 75.1 | 79.8 | 84.0 | 88.8 | 79.5 | 79.6 |

Table 2. Trace element data (ppm)

| | Wehrlite SC74-1W | Wehrlite SH76-2F | Wehrlite SC73-2 | Wehrlite KH73-1 | Wehrlite KH76-1 | Wehrlite SD72-1 | Harzburgite SC74-1H | Spinel Lherzolite SH76-2L | Poikilitic Wehrlite SC73-3 | Poikilitic Wehrlite SC73-6 |
|----|---------------------|---------------------|--------------------|--------------------|--------------------|--------------------|------------------------|---------------------------------|----------------------------------|----------------------------------|
| La | 0.51 | 1.00 | 3.40 | 2.94 | 3.40 | 12.1 | 0.08 | 0.56 | 1.39 | 1.52 |
| Ce | - | 3.2 | 11.3 | 9.9 | 10.8 | 27.6 | - | 1.4 | 4.4 | 5.0 |
| Sm | 0.56 | 1.57 | 4.14 | 3.35 | 3.58 | 4.17 | 0.095 | 0.135 | 0.95 | 1.40 |
| Eu | 0.191 | 0.54 | 1.30 | 1.00 | 1.14 | 1.25 | 0.040 | 0.052 | 0.299 | 0.44 |
| Tb | 0.13 | 0.40 | 0.81 | 0.51 | 0.69 | 0.56 | - | 0.034 | 0.13 | 0.21 |
| Yb | 0.44 | 1.53 | 2.01 | 1.57 | 1.52 | 0.89 | 0.11 | 0.24 | 0.44 | 0.63 |
| Zu | 0.073 | 0.26 | 0.288 | 0.216 | 0.202 | 0.130 | 0.015 | 0.042 | 0.051 | 0.090 |
| Re | 0.35 | 0.99 | 2.47 | 1.76 | 2.08 | 2.40 | 0.05 | 0.06 | 0.54 | 0.94 |
| Ta | 0.21 | 0.23 | 0.57 | 0.40 | 0.40 | 1.23 | 0.39 | 0.19 | 0.46 | 0.27 |
| Th | 2.2 | 1.8 | 3.0 | 2.6 | 2.6 | 3.5 | 1.3 | 1.4 | 1.7 | 0.18 |
| Sc | 22.2 | 51 | 50 | 59 | 49 | 35.5 | 7.05 | 12.0 | 20.7 | 29.4 |
| Co | - | - | - | - | - | - | - | - | - | 124 |
| Cr | 3250 | 2310 | 680 | 44 | 110 | 1320 | 2390 | 2430 | 1080 | 1070 |
| Ni | 660 | 550 | 640 | 630 | 290 | 480 | 2030 | 1970 | 1390 | 1220 |

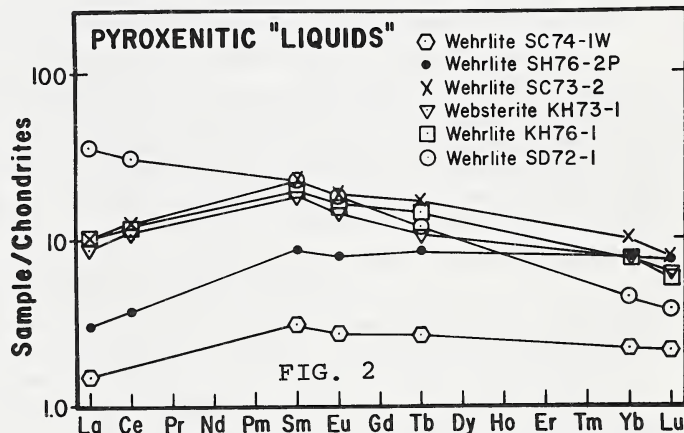


FIG. 2

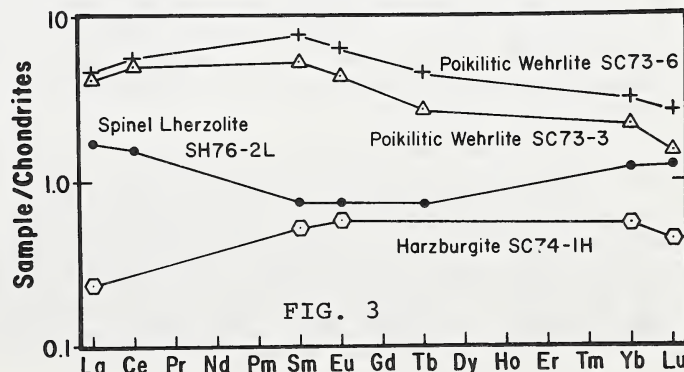


FIG. 3